applied sciences

MDPI

Article

Adam Bayesian Gaussian Process Regression with Combined Kernel-Function-Based Monte Carlo Reliability Analysis of Non-Circular Deep Soft Rock Tunnel

Jiancong Xu [1,2,*], Ziteng Yan [2] and Yongshuai Wang [2]

[1] Key Laboratory of Geotechnical and Underground Engineering of Ministry of Education, Tongji University, Shanghai 200092, China
[2] Department of Geotechnical Engineering, Tongji University, Shanghai 200092, China; 2232538@tongji.edu.cn (Z.Y.); 2232537@tongji.edu.cn (Y.W.)
* Correspondence: xjc1008@tongji.edu.cn

Abstract: Evaluating the reliability of deep soft rock tunnels is a very important issue to be solved. In this study, we propose a Monte Carlo simulation reliability analysis method (MCS–RAM) integrating the adaptive momentum stochastic optimization algorithm (Adam), Bayesian inference theory and Gaussian process regression (GPR) with combined kernel function, and we developed it in Python. The proposed method used the Latin hypercube sampling method to generate a dataset sample of geo-mechanical parameters, constructed combined kernel functions of GPR and used GPR to establish a surrogate model of the nonlinear mapping relationship between displacements and mechanical parameters of the surrounding rock. Adam was used to optimize the hyperparameters of the surrogate model. The Bayesian inference algorithm was used to obtain the probability distribution of geotechnical parameters and the optimal surrounding rock mechanical parameters. Finally, the failure probability was computed using MCS–RAM based on the optimized surrogate model. Through the application of an engineering case, the results indicate that the proposed method has fewer prediction errors and stronger prediction ability than Kriging or XGBoost, and it can significantly save computational time compared with the traditional polynomial response surface method. The proposed method can be used in the reliability analysis of all shapes of tunnels.

Keywords: soft rock tunnel; reliability analysis; Adam; Bayesian inference; Gaussian process regression; Monte Carlo simulation

check for updates

Citation: Xu, J.; Yan, Z.; Wang, Y. Adam Bayesian Gaussian Process Regression with Combined Kernel-Function-Based Monte Carlo Reliability Analysis of Non-Circular Deep Soft Rock Tunnel. *Appl. Sci.* **2024**, *14*, 7886. https://doi.org/10.3390/app14177886

Academic Editors: Junho Chun, Won-Hee Kang, Andrea L. Rizzo and Giuseppe Lacidogna

Received: 17 July 2024
Revised: 13 August 2024
Accepted: 2 September 2024
Published: 5 September 2024

Copyright: © 2024 by the authors. Licensee MDPI, Basel, Switzerland. This article is an open access article distributed under the terms and conditions of the Creative Commons Attribution (CC BY) license (https://creativecommons.org/licenses/by/4.0/).

1. Introduction

The disasters that may occur during the excavation and construction of deep soft rock tunnels include the large deformation of soft rock, large collapse, sand burst collapse, high ground temperature, large water inflow, and so on. Large deformation of soft rock, high ground temperature, and large water influx are some common geological hazards encountered during the construction of deep soft rock tunnels. Large deformation of soft rock, large collapse, and sand burst collapse are often caused by improper construction methods, inadequate advance prediction and forecasting, and failure to discover adverse geological conditions.

The deformation caused by the excavation of deep soft rock tunnels leads to significant unpredictability and uncertainty. Therefore, it is essential to quantitatively assess the disaster risks of deep soft rock tunnels using reliability theory. Using reliability analysis may be more reasonable to deal with the uncertainty and randomness of geotechnical parameters. Therefore, there have been many studies on the reliability of underground structure engineering in recent years [1–7].

A reliability analysis of deep circular tunnels reinforced with fully grouted bolts using a homogenization method was performed employing the first-order reliability method

(FORM) and Monte Carlo simulation (MCS) [8]. The effects of the uncertainty of time-dependent mechanical properties of rock on the failure probability of a tunnel for a period of 100 years are studied by introducing the closed-form solution for a deep circular tunnel excavated within the viscoelastic Burger rock and supported by a double-layer concrete/compressible material, into the active learning reliability analysis method combining Kriging and MCS [9]. Through introducing the creep-damage theory, a time-variant reliability analysis procedure via the probability density evolution method is proposed for deep circular tunnels against delayed failure [10].

The commonly used structural reliability analysis methods include the stochastic reliability method, the response surface method, the first-order method [6,7], and the second-order method in underground engineering [11–14]. In addition, there are other innovative reliability analysis methods in tunnel engineering [15]. Surrogate numerical modelling techniques have recently been used to alleviate the computational burden and produce global response approximations. Surrogate models based on the augmented radial basis functions [16], hybrid particle swarm optimization neural network [17], XGBoost v1.4.0 [18,19], and Bayesian entropy Gaussian process [20] have been used to evaluate the reliability of tunnels. The Kriging model is a Gaussian regression model with no parameters, which was used to calculate the reliability of tunnel engineering [3,21,22]. The reliability method in the framework of the Bayesian model update of the structural dynamic models using measured responses was implemented for high-dimensional model parameter spaces [23]. The system reliability of tunnels reinforced by rock bolts was analyzed through artificial neural networks and the improved hybrid method of the linear response surface method [24].

With further studies on the uncertainty in tunnel and underground engineering, reliability methods have been gradually applied. However, from the above analysis, we note that the reliability study in tunnel engineering of deep soft rock is still in the early stages, and most of the existing tunnel reliability calculation methods are proposed for circular tunnels [25]. These reliability methods make it difficult to evaluate large deformation disaster risks of non-circular deep soft rock tunnels.

Using machine learning methods to establish a surrogate model of the nonlinear mapping relationship between geotechnical parameters and their responses such as displacement and support resistance of tunnels can significantly reduce the time needed for numerical calculations [26]. However, there are currently few studies on the machine learning-based reliability calculation in deep soft rock tunnel engineering. Therefore, the reliability of deep soft rock tunnels needs to be further studied based on machine learning algorithms such as Gaussian process regression (GPR).

In Ref. [8], we proposed the NSGA–III–XGBoost based stochastic reliability analysis method for deep soft rock tunnels. The NSGA–III–XGBoost method uses the Latin hypercube sampling method to generate dataset samples of geo-mechanical parameters and adopts XGBoost to establish a model of the nonlinear relationship between displacements and surrounding rock mechanical parameters. And NSGA–III is used to optimize the surrogate model hyperparameters. Finally, the failure probability is computed by the optimized surrogate model. The advantages of the NSGA–III–XGBoost method were demonstrated through a comparison between the support vector regression method and the backpropagation neural network method.

In this study, an Adam–Bayesian–Gaussian process regression (ABGPR) with combined kernel-function-based Monte Carlo simulation reliability method (ABGPR–MCSRM) is proposed to assess the reliability of non-circular deep soft rock tunnels. The Latin hypercube sampling (LHS) method is adopted to obtain the geo-mechanical parameter dataset sample for the reliability analysis of a deep soft rock tunnel. Three combined kernel functions of the Gaussian process regression algorithm (GPRA) are constructed and compared with the existing basic kernel functions to select the kernel function with more accurate and effective reasoning and learning. Then, the surrogate model of numerical simulation is constructed using GPRA, and the adaptive momentum (Adam) algorithm

is used to optimize the hyperparameters of the surrogate model. And the probability distribution of geotechnical parameters and the optimal surrounding rock mechanical parameters are obtained by using the Bayesian inference algorithm. Finally, the tunnel reliability is calculated using the Monte Carlo simulation reliability method (MCSRM) through the ABGPR-based optimal surrogate model. The advantages of the proposed method are demonstrated through a comparison between the NSGA–III–XGBoost-based method and the Kriging-based method.

The purpose of this study is to provide some novel insights for the probabilistic reliability analysis of deep soft rock tunnels more rationally. The main contribution of this study is that we construct a combinatorial kernel function, which can be used for more accurate and effective reasoning and learning. We also establish a more accurate ABGPR-based numerical surrogate model than the proposed surrogate model in Ref. [8], which can provide a high-precision probabilistic reliability evaluation method (ABGPR–MCSRM) of deep rock tunnel engineering with fewer prediction errors and stronger prediction ability than the NSGA–III–XGBoost-based method or the Kriging-based method.

The research is organized as follows: i. the Adam–Bayesian–GPR-based MC (ABGPR–MCS) reliability calculation procedure framework is implemented in Section 2; ii. Section 3 presents one engineering example for verifying the feasibility, validity, and advantages of the proposed framework; iii. the conclusion is presented in Section 4.

2. Adam–Bayesian–GPR-Based MC Reliability Calculation Procedure Framework

2.1. Performance Function of Surrounding Rock Primary-Support Structure System

Based on the design specification of the perimeter deformation of a deep-buried soft rock tunnel, the performance function of the surrounding-rock initial support structure system is given by Formula (1).

$$g_{\text{Tunnel}}(\boldsymbol{X}) = u_{\max} - u(\boldsymbol{X}) \tag{1}$$

where $u_{\max}$ is the design value of tunnel displacement; $u(\boldsymbol{X})$ is the calculation value of tunnel displacement corresponding to $\boldsymbol{X}$; $\boldsymbol{X}$ is the random variable vector, that is, surrounding rock mechanical parameters in this study.

In addition to satisfying tunnel clearance and structural dimensions, an adequate amount of deformation should be reserved after tunnel initial support on designing a tunnel's excavation section. The size of the design reserved deformation can be obtained by tunnel surrounding rock classification, buried depth, section size, support conditions, construction method, etc. Some adjustments are sometimes based on the results of in situ monitoring. Based on the Chinese Highway Tunnel Design Code (CHTDC), tunnel reserved deformation is generally 5~20 cm.

When designing based on the bearing capacity, the allowable vault settlement and allowable convergence of the tunnel initial support structure with composite lining should be determined by tunnel rock classification, surrounding rock geological conditions, and buried depth. Based on the CHTDC, it is generally 0.1~3.0% of the tunnel's maximum clearance size.

2.2. Gaussian Process Regression

The Gaussian process (GP) [27] is a type of general supervised learning algorithm that can be used to solve both regression and classification problems. Gaussian process regression (GPR) can implement training on input data to predict the value of unknown data. It can obtain the probability distribution of prediction values, different from the deterministic machine learning algorithm. The empirical confidence interval can be calculated accordingly, which can take into better account the influence of system uncertainty. The GPR steps are presented as follows:

Step 1: Calculate the kernel function and mean function of GP. The mean function is often set to 0 or the average value of training data, and the kernel function is selected based on the actual situation, as denoted in Formula (2). The hyperparameters of the GPR model

can be determined by the optimization algorithms, such as the Adam algorithm [28] and the maximum likelihood estimation (MLE) method.

$$\boldsymbol{K} = \begin{bmatrix} k(x_1,x_1) & k(x_1,x_2) & \cdots & k(x_1,x_n) \\ k(x_2,x_1) & k(x_2,x_2) & \cdots & k(x_2,x_n) \\ \vdots & \vdots & \ddots & \vdots \\ k(x_n,x_1) & k(x_n,x_2) & \cdots & k(x_n,x_n) \end{bmatrix} \tag{2}$$

Step 2: According to the properties of Gaussian distribution, for the to-be-predicted (x_*, y_*), Formula (3) is obtained by Gaussian distribution.

$$\begin{bmatrix} y \\ y_* \end{bmatrix} \sim \mathcal{N}\left(0, \begin{bmatrix} \boldsymbol{K} & \boldsymbol{K}_*^T \\ \boldsymbol{K}_* & \boldsymbol{K}_{**} \end{bmatrix}\right) \tag{3}$$

where $\boldsymbol{K}_* = [k(x_*,x_1)k(x_*,x_2) \cdots k(x_*,x_n)]$; $K_{**} = k(x_*,x_*)$; $y_j(j = 1,2,\ldots,M)$ is the response of $x_i(i = 1,2,\ldots,n)$.

Step 3: The posterior probability is calculated using the Bayesian inference theory, and the relationship between the predicted value and actual value $\boldsymbol{y}$ is denoted by Formula (4).

$$y_* \Big| \boldsymbol{y} \sim \mathcal{N}\left(\boldsymbol{K}_*\boldsymbol{K}^{-1}\boldsymbol{y}, K_{**} - \boldsymbol{K}_*\boldsymbol{K}^{-1}\boldsymbol{K}_*^T\right) \tag{4}$$

Therefore, the mean $\overline{y}_* = \boldsymbol{K}_*\boldsymbol{K}^{-1}\boldsymbol{y}$, and the variance $\mathrm{var}(y_*) = K_{**} - \boldsymbol{K}_*\boldsymbol{K}^{-1}\boldsymbol{K}_*^T$.

Step 4: Substitute the to-be-predicted data and calculate the predicted value using Formula (4).

2.3. Bayesian Inference

The Bayesian method [28] is adopted to update the probability of the hypothesis to obtain more information, as shown in Formula (5).

$$p(\theta|X,\alpha) = \frac{p(X|\theta,\alpha)p(\theta|\alpha)}{p(X|\alpha)} \propto p(X|\theta)p(\theta|\alpha) \tag{5}$$

where X represents a set of observation points $x_i(i = 1,2,\cdots,n)$; θ denotes the parameters of the distribution corresponding to a data point set.

In Bayesian inference [29], $p(\theta|\alpha)$ is customarily referred to as the prior distribution of parameters in the absence of any observation data. The observation data distribution under a specific parameter $p(X|\theta,\alpha)$ is referred to as the likelihood function. The likelihood function can also be abbreviated as $L(\theta|X)$ or $p(X|\theta)$ because θ obeys the probability distribution with α.

After considering the distribution of all possible parameters θ for the observation data, the marginal distribution $p(X|\alpha)$ is referred to as the marginal likelihood function. After considering the observation data, the parameter distribution $p(\theta|X,\alpha)$ is referred to as the posterior distribution. Therefore, Bayesian inference can also be denoted as the posterior distribution being proportional to the prior distribution multiplied by the likelihood function. Its posterior distribution can be denoted by Formula (6) when given a new observation point $\widetilde{x}$.

$$p(\widetilde{x}\Big|X,\alpha) = \int p(\theta|X,\alpha)p(\widetilde{x}|\theta)\,d\theta \tag{6}$$

2.4. Bayesian Update of Geo-Mechanical Parameters

The Bayesian update of geo-mechanical parameters involves prior distribution, likelihood function, and posterior distribution. Prior information mostly relates to the estimations made before the collection of monitoring data, such as the assumed distribution of

geo-mechanical parameters based on geological survey reports, the experience of comparable projects, expert views, and so on.

The posterior distribution mainly adopts the machine learning algorithm to carry out the numerical simulation with the prior information or updates the range of geo-mechanical parameters in real time using the field monitoring information. After the Bayesian inference each time, the posterior distribution of geo-mechanical parameters automatically becomes the prior distribution of the next inference, and so on.

2.5. GPR-Based Relationship between Displacement and Geo-Mechanical Parameters

In this study, the GPR model was used to surrogate the numerical model and to map the nonlinear relationship between monitored displacements and geo-mechanical parameters, such as elastic modulus, internal friction angle, cohesion, and Poisson's ratio, which greatly reduces the computing time. We used the Bayesian method to obtain the probabilistic distribution law for the uncertainty in geo-mechanical parameters.

The mathematical model $GPR(\boldsymbol{X})$ is denoted by Formula (7).

$$\begin{cases} GPR(\boldsymbol{X})\text{: } \boldsymbol{R}^N \rightarrow \boldsymbol{R}^M \\ \boldsymbol{Y} = GPR(\boldsymbol{X}) \end{cases} \tag{7}$$

where $\boldsymbol{X} = (\boldsymbol{x}_1, \boldsymbol{x}_2, \ldots, \boldsymbol{x}_N)$, $\boldsymbol{x}_i$ $(i = 1, 2, L, N)$ are a vector of geo-mechanical parameters such as elastic modulus, internal friction angle, cohesion and Poisson's ratio, etc.; N is the dimension of geo-mechanical parameters; $\boldsymbol{Y} = (y_1, y_2, \ldots, y_M)$ is an M dimensional vector of displacement. In this study, the observable output is the displacement; correspondingly, M denotes the dimension of displacement.

To obtain $GPR(\boldsymbol{X})$, the necessary training samples are constructed by combining numerical analysis (e.g., a finite element method (FEM) model) and test design, which is used to obtain tunnel displacements according to a given set of geo-mechanical parameters. Compared with other sampling design methods, the Latin hypercube sampling (LHS) method is always comprehensive in considering the marginal small-probability events in the test. Therefore, LHS is more suitable for large-scale numerical test sampling. In this study, LHS is adopted to obtain the samples of geo-mechanical parameters, and these geo-mechanical parameters are taken as the input of GPR. The displacement is taken as the output of GPR.

2.6. Combined Kernel Function Construction and Selection

GPR defines the homogeneity difference between different observation data as a kernel function, which not only defines a general kernel function but also allows us to customize the kernel function according to different problems. The selection of a kernel function is the key to ensuring the accuracy of GPR.

The GPR-based reliability analysis largely depends on the selected covariance function, that is, the quality of the kernel function. The basic idea of the kernel function is to map the undivided data in the low-dimensional space to the high-dimensional space to achieve effective separation. In this study, we investigate the influence of different commonly used kernel functions on the calculation results of GPR and build combined kernel functions for more accurate and effective thinking and learning.

Because there is no periodic regression trend in the data in this study, the following basic kernel functions are selected from common kernel functions of GPR [30]: i. radial basis kernel function (*RBF*) (see Formula (8)); ii. Matern kernel function denoted by Formula (9); iii. Matern kernel function of v = 1.5 (*K1.5*, see Formula (10)); iv. Matern kernel function of v = 2.5 (*K2.5*, see Formula (11)).

$$K_{\mathrm{RB}}(x, x') = \exp\left(-\frac{\|d\|^2}{2l^2}\right) \tag{8}$$

$$K_{Matern}(x, x') = \frac{2^{1-v}}{\Gamma(v)}\left(\frac{\sqrt{2v}|d|}{l}\right)^{v} K_v\left(\frac{\sqrt{2v}|d|}{l}\right) \tag{9}$$

$$K_{\text{Matern},1.5}(x, x') = \left(1 + \frac{\sqrt{3}|d|}{l}\right)\exp\left(-\frac{\sqrt{3}|d|}{l}\right) \tag{10}$$

$$K_{\text{Matern, }2.5}(x, x') = \left(1 + \frac{\sqrt{5}|d|}{l} + \frac{5|d|^2}{3l^2}\right)\exp\left(-\frac{\sqrt{5}|d|}{l}\right) \tag{11}$$

where x, x' are the input data of the training sample and the input data of the test sample, respectively; d is Euclidean distance; l is the length scaling factor, which controls the fluctuation degree, and its default value is 1.0; v is the parameter used to control the smoothness of the resulting function, and the common value in the field of machine learning is v = 1.5 or 2.5; $\Gamma(\cdot)$ is the gamma function; $K_{\upsilon}(\cdot)$ is the modified Bessel function of the second kind [31].

Under the sufficient condition that Mercer's theorem of kernel functions is satisfied, the kernel operations of addition and multiplication can be carried out for the above classical kernel functions (see Formulas (8)–(11)), and then the data can be modelled based on the new combined kernel. In order to select the kernel function with the best surrogate model performance, we study the performances of RBF, K1.5, K2.5, and the following combined kernel functions: $RBF + K_{\text{Matern},1.5}(x, x')$ (*RBFK1.5*); $RBF + K_{\text{Matern, }2.5}(x, x')$ (*RBFK2.5*); Constant $\times$ *RBF* (see Formula (12)) (*CRBF*), based on nearly a hundred trial calculations.

$$K_{\text{RBC}}(x, x') = \text{C} \cdot \exp\left(-\frac{\|d\|^2}{2l^2}\right) \tag{12}$$

where C is constant.

2.7. Adam–Bayesian–GPR-Based MCS Reliability Analysis

The whole calculation process of the Adam–Bayesian–GPR-based MCS reliability analysis method is depicted in a flowchart in Figure 1. The detailed steps are as follows.

Step 1: Generate a dataset of geo-mechanical parameters using the LHS method.

Step 2: Use the finite element method (FEM) such as ABAQUS 2020 to calculate the displacement of the tunnel at each monitoring point.

Step 3: Establish the surrogate model by GPR training on the dataset:

First, the original data of geo-mechanical parameters and displacements are preprocessed centrally and standardized to form the sample dataset;

Second, select the appropriate kernel function based on the actual situation;

Third, establish the model to map the nonlinear relationship between displacements and their corresponding geo-mechanical parameters;

Finally, the hyperparameters of the GPR model are determined by the Adam algorithm and provide the optimal surrogate model. The Adam algorithm has become the mainstream method in the field of stochastic gradient optimization, with the advantages of easy implementation, low memory consumption, and high computational efficiency. It is very suitable for situations with large datasets and parameters. Therefore, the Adam algorithm is selected to tune the hyperparameters of the surrogate model established using GPR in this study.

Given the set of observations $\boldsymbol{y}^*$ in the test sample dataset, Adam is used to learn the hyperparameters $\boldsymbol{\theta}$ (the parameter $\boldsymbol{\theta}^x$ of $\boldsymbol{k}_*^x$) to maximize the marginal likelihood $p(\boldsymbol{y}^*|\boldsymbol{X}, \boldsymbol{\theta}^x)$. Here, $\boldsymbol{k}_*^x$ is the vector of covariances between the test point $\boldsymbol{x}^*$ and training points, and σ_n^2 is the variance of the GPR-based model.

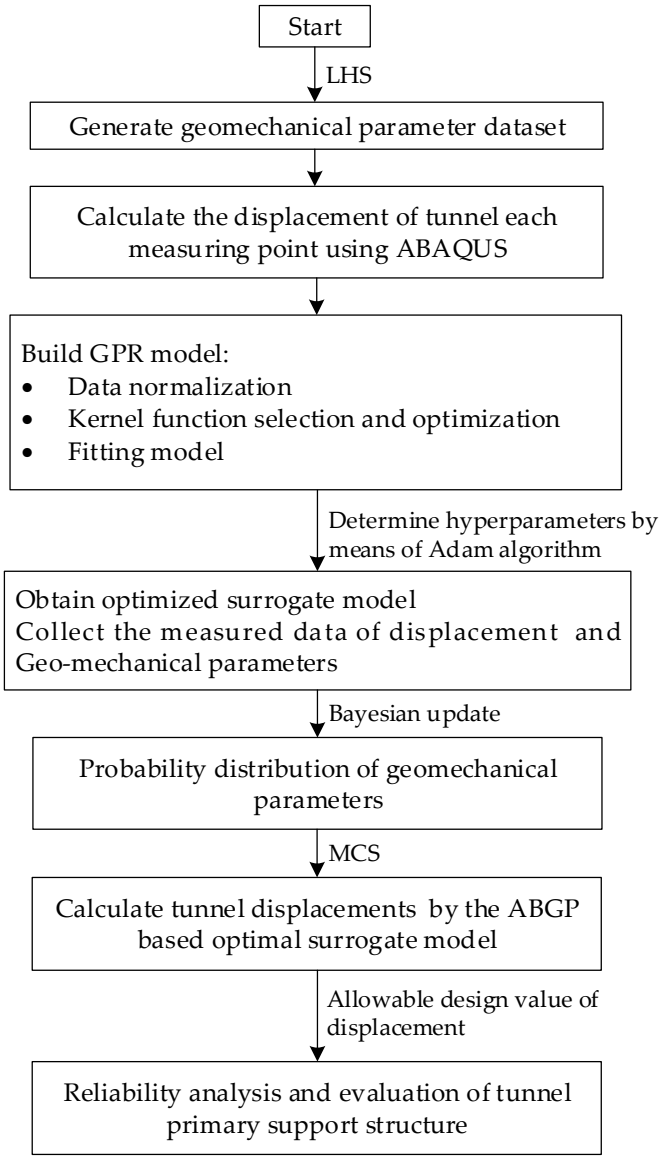

Figure 1. Calculation procedure of ABGPR–MCS reliability analysis.

Step 4: The posterior probability of geo-mechanical parameters is calculated using the Bayesian inference theory. The mean and variance of the predicted value of geo-mechanical parameters are obtained by Formula (4).

Step 5: Random sampling using the LHS method is carried out based on the mean and variance of geo-mechanical parameters obtained in Step 4. Then, the displacements of the tunnel are calculated by the optimal ABGPR-based surrogate model.

Step 6: Using the Monte Carlo simulation (MCS) reliability analysis method, we calculate the failure probability of tunnel primary support structure using Formula (13).

$$P_{\mathrm{f}} \approx \frac{N_{\mathrm{f}}}{N} \tag{13}$$

where P_{f} is the failure probability of the tunnel primary support structure; N_{f} is the number of $g^{j}_{\mathrm{Tunnel}}(\boldsymbol{X}) = u_{\max} - u_j(\boldsymbol{X}) < 0$ in all $g^{j}_{\mathrm{Tunnel}}(\boldsymbol{X})(j = 1, 2, \cdots, N)$; N is the total number of random samples.

In this study, our numerical simulation did not take into account dynamic loads and weakening of the rock mass due to the presence of water.

3. Case Study

3.1. Problem Description

In this study, the reliability of a deep soft rock highway tunnel is analyzed using the proposed Adam–Bayesian–GPR-based MCS reliability calculation method. As shown in Figure 2, the horseshoe-shaped highway tunnel with a height of 10.23 m and span of 12.46 m is located in Gansu Province in China. The tunnel's surrounding rock is fully strongly weathered granite gneiss. The design parameters of the tunnel initial support are as follows: non-prestressed rock bolt length ϕ 25–5 = 3.5 m; grille steel frame spacing 25 = 0.6 m; sprayed concrete thickness = 25 cm; steel ϕ eight-mesh spacing = 20 × 20 cm. The design parameter of the tunnel second lining is a reinforcement thickness = 33–45 cm.

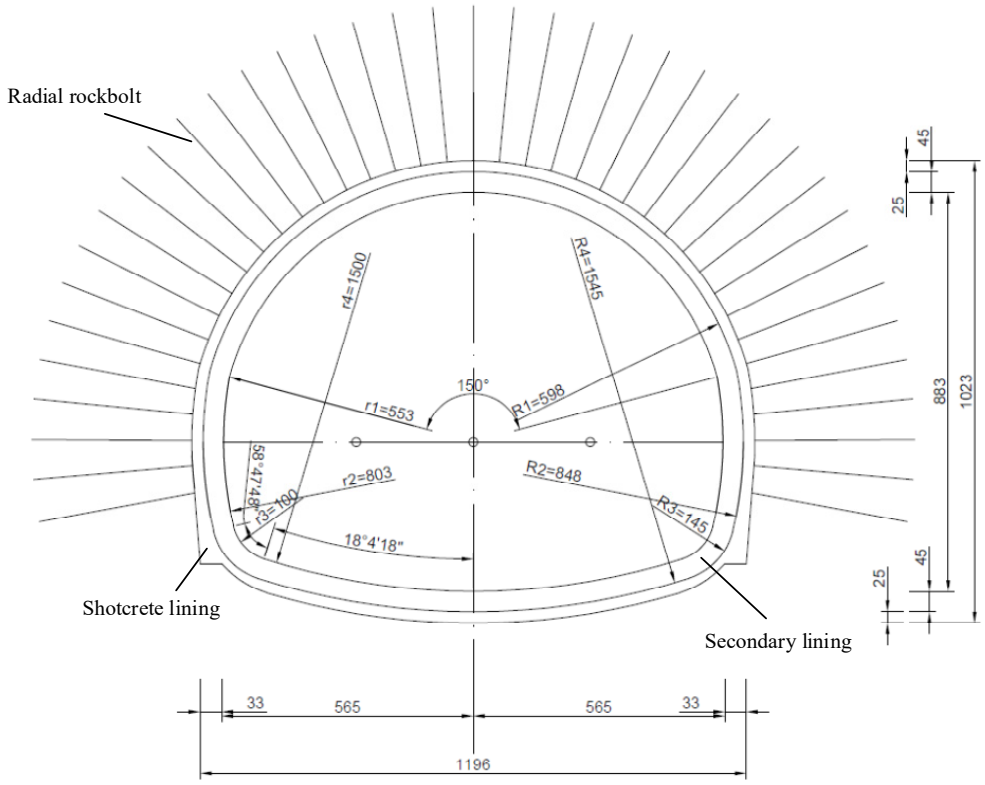

Figure 2. Cross-section of highway tunnel (unit: cm).

The two-dimensional numerical simulation is completed using ABAQUS. The top of the model is taken as a free surface, and both sides of the horizontal direction (X direction) boundaries and bottom boundary are constrained using displacements. In the Y direction (longitudinal direction of the tunnel), a single-layer element is adopted, and the displacement in the Y direction is strictly restricted. Quadrilateral elements are selected for the model. The FEM model is 100 m in the horizontal direction and 149.2 m in the vertical direction, with 5600 nodes and 2736 elements. The horizontal (X direction) lateral pressure of 1.2-times self-weight stress is applied on both sides. A self-weight stress field is applied in the model vertical direction. The lateral pressure coefficient is λ = 1.2; the surrounding-rock bulk density = 24.0 kN/m^3.

The elastic–plastic model and the Mohr–Coulomb yield criterion are adopted to simulate the surrounding rock. The rock-bolt-combined composite concrete lining is installed as a support. The design parameters of the rock bolt, initial support, and second lining are as follows: i. rock bolt Young's modulus E_{bolt} = 210.0 GPa; ii. rock bolt Poisson's ratio ν_{bolt} = 0.3; iii. Young's modulus of grillage steel frame shotcrete E_{IS} = 26.311 GPa; iv. Poisson's ratio of grillage steel frame shotcrete ν_{IS} = 0.22; v. concrete lining Young's modulus E_{CL} = 28.0 GPa; vi. concrete lining Poisson's ratio ν_{CL} = 0.27.

The displacement values of each measurement point or line under varied surrounding-rock parameters are used as the dataset for the proposed method in this study. The layout of monitoring points or lines is shown in Figure 3. The measured data of a section in Table 1 are selected as a representative.

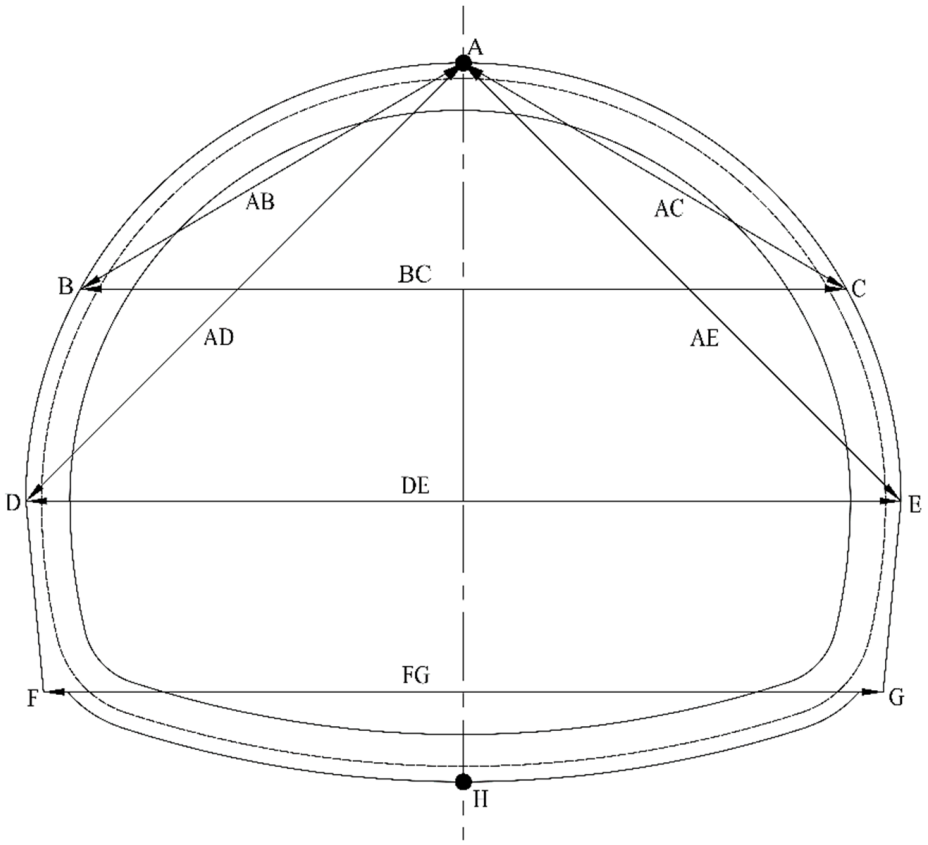

Figure 3. Schematic diagram of tunnel monitoring point layout.

Table 1. On-site monitoring data of a tunnel section.

Measuring Points/Lines	A	H	AB	AC	BC	AD	AE	DE	FG
Monitoring displacement/cm	–9.74	8.43	–6.44	–6.44	–9.99	–9.95	–9.96	–12.59	–10.43

3.2. Performance Function and Random Variables

For simplicity, only the maximum allowable inward displacement of tunnel shotcrete lining is taken as the criterion of its stability. The performance function $G_{\text{Tunnel}}(\boldsymbol{X})$ is obtained using Formula (14). According to the CHTDC, the maximum design value of the vault settlement $u_{\max}$ is taken as u_{vmax} = 0.1 m, and the maximum displacement convergence values $u_{\max}$ of monitoring lines AB, AC, BC, AD, and AE are taken as $u_{\text{ABcmax}} = u_{\text{ACcmax}}$ = 0.075 m, u_{BCcmax} = 0.072 m, and $u_{\text{ADcmax}} = u_{\text{AEcmax}}$ = 0.087 m, respectively.

$$G_{\text{Tunnel}}(\boldsymbol{X}) = u_{\max} - u(E, c, \varphi, \nu) \tag{14}$$

where E is rock Young's modulus; ν is rock Poisson's ratio; φ is rock friction angle; and c is rock cohesion.

E, ν, φ and c are taken as the basic random variables of rock with statistical properties, as shown in Table 2. The properties of initial support, second lining, and rock bolt are assumed to be deterministic.

Table 2. Statistical properties of rock mechanical parameters [7].

Random Variables	Distribution	μ_{X_i}	σ_{X_i}	COV
ν	Normal	0.33	0.033	0.1
$\varphi/^\circ$	Normal	33	4.95	0.15
E/MPa	Normal	350	50.5	0.144
c/kPa	Normal	210	23	0.11

3.3. Kernel Function Selection

The kernel function selection of GPR is generally based on the following considerations:

(1) Data characteristics: The selection of kernel functions should take into account the characteristics of the data, such as dimensionality, linear separability, and the presence of noise.
(2) Model performance: The selection of kernel functions should also be based on the performance requirements of the model. Evaluate the performance of different kernel functions through cross-validation and other methods, and select the kernel function that can provide the best predictive performance. For example, by comparing the training error and testing error of the model, a kernel function that can fit the data well while avoiding overfitting can be selected.
(3) Computational resources: When choosing a kernel function, it is necessary to balance the complexity of the model and computational feasibility.
(4) Parameter adjustments: Kernel functions typically have parameters that need to be adjusted through optimization processes to maximize model performance. Therefore, when selecting kernel functions, optimization algorithms for model hyperparameters should also be considered.

For constructing a GPR-based surrogate model, the model performance is the first and most important consideration among the four above-mentioned considerations of the kernel function selection of GPR.

To quantitatively evaluate the performance of different kernel functions on the proposed algorithm in the test set, the average absolute percentage error (*MAPE*) and the determination coefficient (R2_score) are selected as the prediction and evaluation indices to measure the accuracy of the proposed algorithms. *MAPE* is denoted by Formula (15), and R2_score is expressed by Formula (16).

$$MAPE = \frac{100\%}{n}\sum_{i=1}^{n}\left|\frac{\hat{y}_{\mathbf{p}i} - y_{\mathbf{a}i}}{y_{\mathbf{a}i}}\right| \tag{15}$$

where $\hat{y}_{\mathbf{p}i}$ is prediction value; $y_{\mathbf{a}i}$ is actual value.

$$R2_score = 1 - \frac{\sum_i \left(\hat{y}_{\mathbf{p}i} - y_{\mathbf{a}i}\right)^2}{\sum_i \left(\overline{y}_{\mathbf{a}i} - y_{\mathbf{a}i}\right)^2} \tag{16}$$

where $\overline{y}_{\mathbf{a}i}$ is the mean of actual data.

Through the error analysis of elastic modulus regression results, the evaluation indices of simulation-based data test sets under six different kernel functions (*RBF*, *K1.5*, *K2.5*, *RBFK1.5*, *RBFK2.5* and *CRBF*) were compared, as shown in Figure 4.

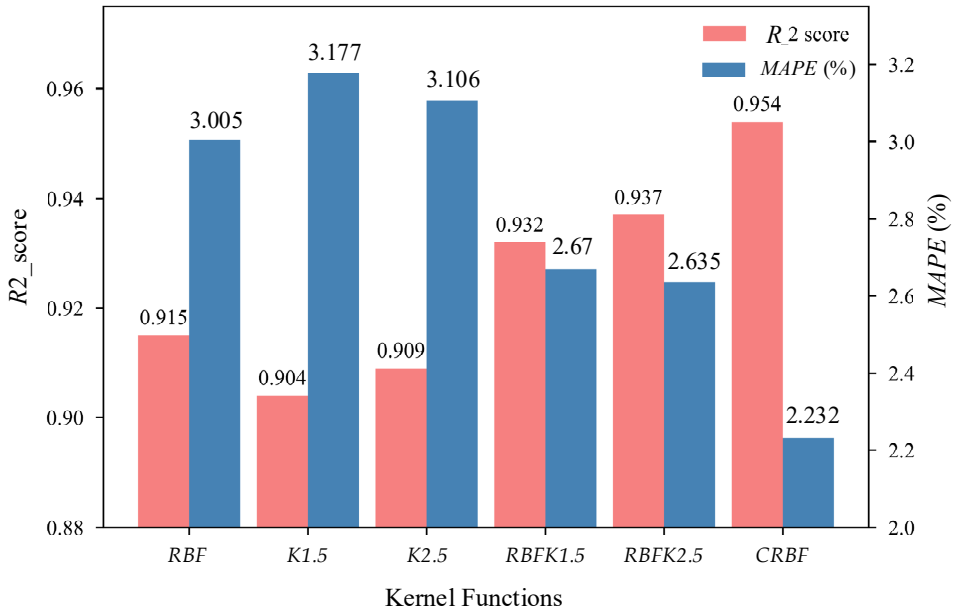

Figure 4. *R*2_score values corresponding to different kernel functions.

From Figure 4, we note that the kernel function with the strongest prediction ability is CRBF, whose *R*2_score index is 0.954 and *MAPE* is only 2.232%. It is noted that the prediction ability of the model was greatly improved through the design of the combined kernel function. Therefore, CRBF is selected as the kernel function in the proposed Adam–Bayesian–GPR-based MCS reliability analysis.

In the CRBF combined kernel function, the complexity and fitting ability of the RBF-based model can be balanced by adjusting the weight of the constant kernel function (C) to adapt to different data distributions and model requirements. The two hyperparameters of constant kernel function (C) and length scaling factor (l) in the CRBF combined kernel function can be determined using the Adam algorithm.

3.4. Results and Discussion

3.4.1. ABGPR–MCS Reliability Analysis Results

Firstly, the geo-mechanical parameters in Table 2 were sampled 1000 times by the Latin hypercube method. Secondly, these 1000 sample sets are substituted into the FEM model, and simulation calculations are performed to obtain the corresponding displacement data of each monitoring point in Figure 3. Third, the proposed ABGPR algorithm is used to establish one model to surrogate the numerical calculation. Finally, we enter and update the optimized surrogate model with the displacement data from each measurement site in Table 1 to produce the appropriate mean value, variance, and confidence interval of geo-mechanical parameters, as shown in Table 3.

Table 3. Calculation results of surrounding-rock mechanical parameters.

Parameters	*E*/GPa	μ	*c*/MPa	φ/°
Mean	0.3306	0.338	0.1896	32.795
Standard deviation	0.001875	0.001	0.001775	0.17575
Confidence interval of 95%	[0.3269, 0.3344]	[0.336, 0.340]	[0.1860, 0.1931]	[32.444, 33.147]

Each FEM simulation calculation time using ABAQUS (three-step construction method, excavation length 12 m and each excavation length 1 m) is about 1 h, while the calculation time of the surrogate model is generally only 30~40 s.

On using the ABGPR–MCS reliability analysis method, it is first necessary to set the maximum number of tests. The amount of random sampling of parameters should be determined in combination with the target failure probability of the tunnel engineering. Assuming that the failure probability P_f of the tunnel is 0.5% and the error level is 0.1, the total number of random samples N is 20,000, obtained using Formula (17) [32].

$$N > \left(\frac{1}{P_f} - 1\right) \cdot 10^2 \approx \frac{10^2}{P_f} \tag{17}$$

According to the statistical parameters of the surrounding rock in Table 3, 30,000 rounds of random sampling are carried out via the MCS method. A frequency distribution histogram is generated by the statistical analysis of sampling results, as shown in Figure 5. Comparing the randomly generated parameter sample values with the fitted normal curve, we note from Figure 5 that the statistical parameters conform to the normal distribution of the original inversion results. It can be concluded that the random sampling of each group meets the requirements of the ABGPR–MCS algorithm.

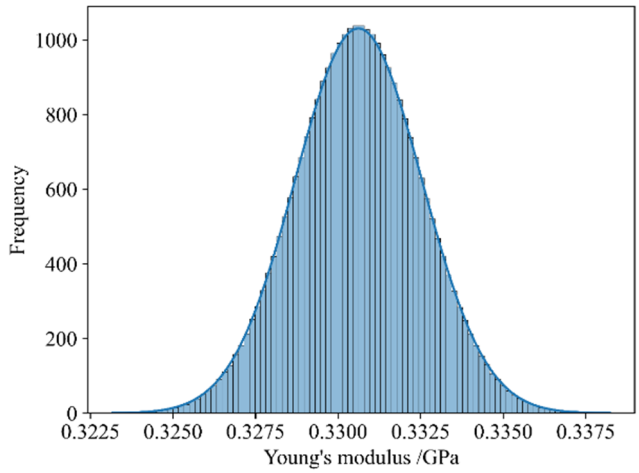

(**a**) Frequency distribution of Young's modulus

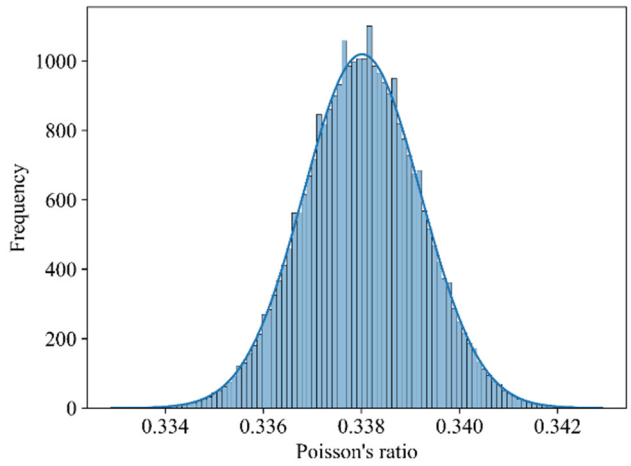

(**b**) Frequency distribution of Poisson's radio

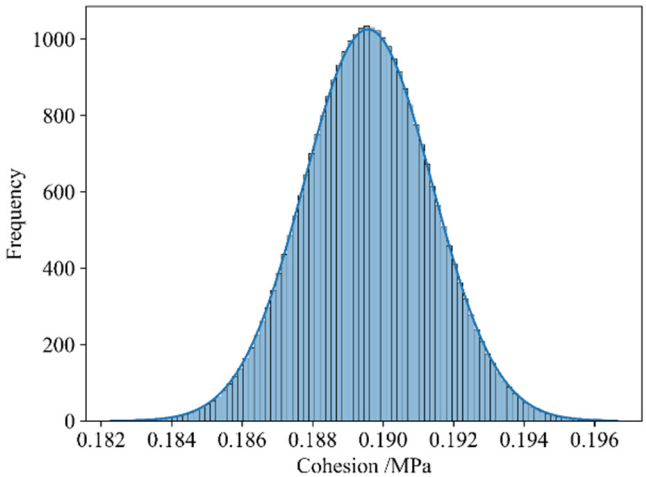

(**c**) Frequency distribution of cohesion

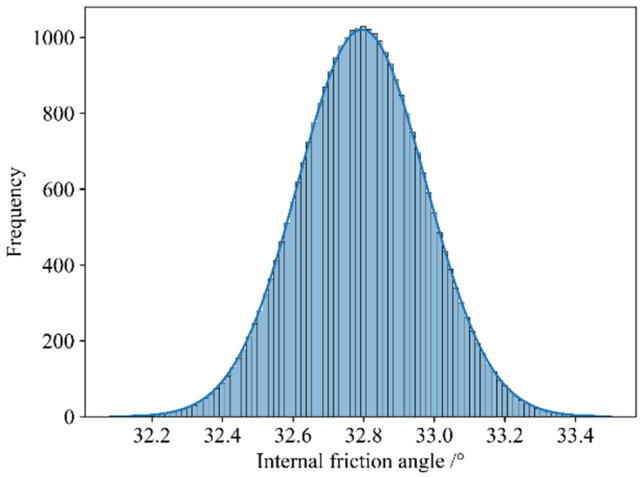

(**d**) Frequency distribution of internal friction angle

Figure 5. Frequency distribution histogram of surrounding-rock parameters.

The substitution of FEM simulation for tunnel excavation and support was completed on the above-mentioned 30,000 sets of geo-mechanical parameters using the optimized sur-

rogate model used by Python 3.7, respectively, to obtain the corresponding vault settlement and horizontal displacement data of the tunnel.

For monitoring point A, based on the performance function of the initial support structure $Z = 0.1 - u_v$ denoted by Formula (14), the number of $Z < 0$ is 55, and the number of $Z > 0$ is 29,945; using the approximate probability method and Formula (13), its failure probability is 0.1833%, and its reliability index is 2.906. In the same way, we can obtain the reliability indices of measuring lines BC, AB, AC, AD, and AE, respectively, as 3.004, 2.713, 2.713, 2.734, and 2.734.

3.4.2. Comparison of Numerical Calculation and Surrogate Model Calculation Based on ABGPR, Kriging, and XGBoost for Monitoring Point Displacement

From Figure 6, we note that for monitoring points A, E, and H, the displacement calculation values of each monitoring point based on the ABGPR surrogate model are relatively close to their numerical calculation values, while the error based on the XGBoot surrogate model is the largest. The error based on the Kriging surrogate model is between the error based on the ABGPR surrogate model and the error based on the XGBoot surrogate model.

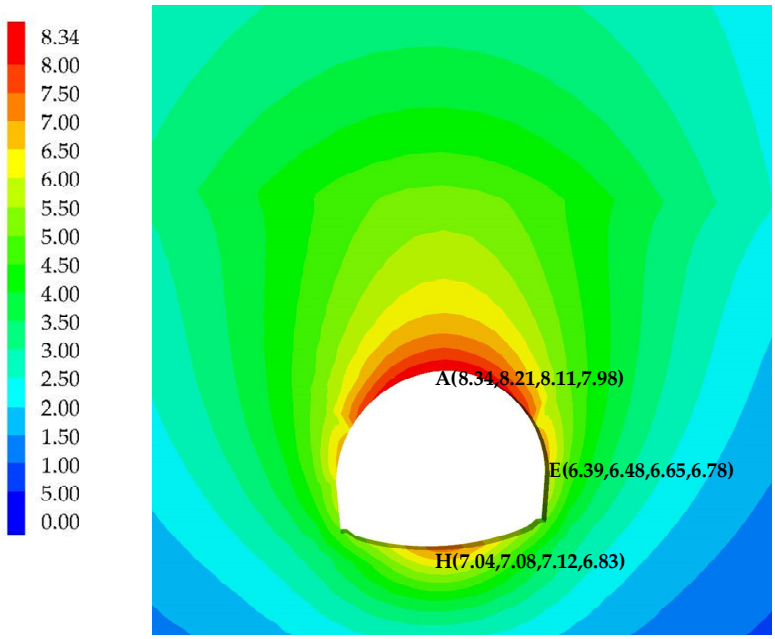

Figure 6. Comparison of numerical calculation and surrogate model calculation for monitoring point displacement (Unit: cm). Note: The numbers in parentheses for each monitoring point in Figure 6 represent the numerical calculated values and surrogate model calculation values based on ABGPR, Kriging, and XGBoost, respectively.

3.4.3. Comparison of Tunnel Reliability Based on ABGPR, Kriging, and XGBoost

The specific parameter values used by ABGPR, Kriging, and XGBoost in this study are as follows, respectively.

(1) ABGPR parameter values: constant kernel function (C) = 30.5^2, length scaling factor (l) = 0.0882.
(2) The DACE [33] (Design and Analysis o I Computer Experiments) toolbox function [dmodel. perf] = dacefit (S, Y, regr, corr, theta) in MATLAB is used to construct Kriging surrogate model. Kriging parameter values: theta = 1.
(3) XGBoost parameter values: max_depth = 1, learning_rate = 0.5, n_estimators = 4000, gamma = 0.

The kernel function used in ABGPR is denoted by Formula (12). The covariance function used in the Kriging surrogate model is denoted by Formula (18).

$$K_{\text{Kriging}}(x, x') = \exp\left(-\frac{1}{2}(x - x')^{\mathrm{T}}\Lambda^{-1}(x - x')\right) \tag{18}$$

where $\Lambda = \text{diag}(\lambda_1, \lambda_2, \ldots, \lambda_m)$.

The convergence criteria for the surrogate models based on ABGPR, Kriging, and XGBoost are as follows: if there is no underfitting or overfitting, it can be considered that the surrogate model has converged when the change in the loss function value of the surrogate model is very small (such as less than 0.001) or fluctuates within a small range.

Using the same sample dataset as the ABGPR calculation, the nonlinear mapping surrogate models between geo-mechanical parameters and tunnel displacement or convergence response are constructed by using the ABGPR, Kriging, and XGBoost algorithms, respectively. Using these optimized surrogate models, the displacement or convergence values of point A, line BC, AB, AC, AD and AE are obtained, corresponding to 30,000 sets of geo-mechanical parameters generated by the MCS method. For point A, line BC, AB, AC, AD and AE, the *R*2_score indices and MPAE of optimized surrogate models based on ABGPR, Kriging, and XGBoost are shown in Figures 7 and 8, respectively, and their reliability indices are calculated by Formulas (14) and (15), as shown in Figure 9.

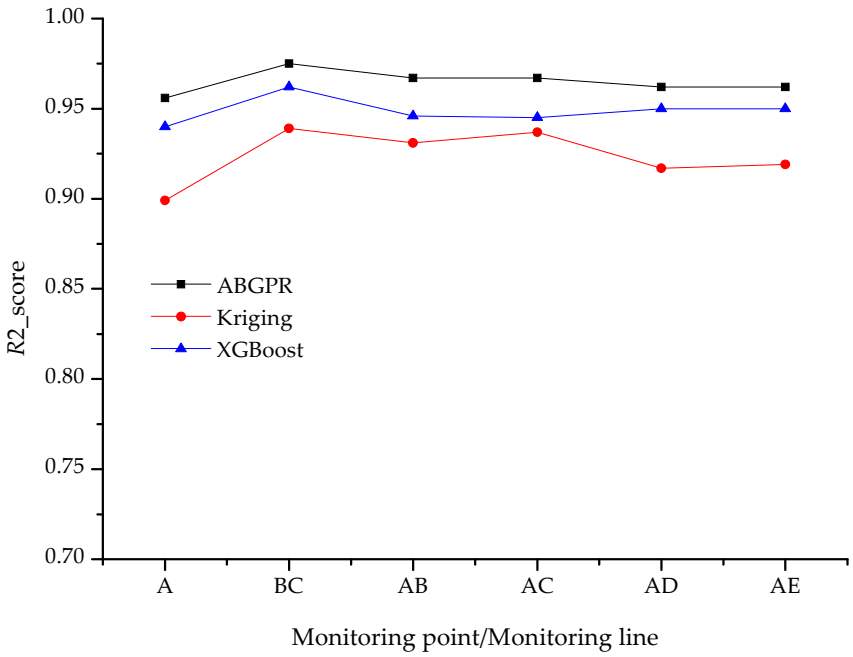

Figure 7. Comparison of *R*2 for models based on ABGPR, Kriging and XGBoost.

From Figure 7, we note that for monitoring point A and monitoring lines BC, AB, AC, AD and AE, the *R*2_score indices of ABGPR-based surrogate models are all greater than 0.956 and fluctuate between 0.956 and 0.975; the *R*2_score indices of Kriging-based surrogate models fluctuate between 0.899 and 0.939; the *R*2_score indices of XGBoost-based surrogate models fluctuate between 0.94 and 0.962. Furthermore, the ABGPR-based *R*2_score index of each measuring point/line is greater than that based on Kriging or XGBoost. The fluctuation in ABGPR-based *R*2_score values (0.019) is the least among them, which is close to that of XGBoost-based *R*2_score values (0.022), and that of Kriging-based *R*2_score values (0.04) is the largest among them.

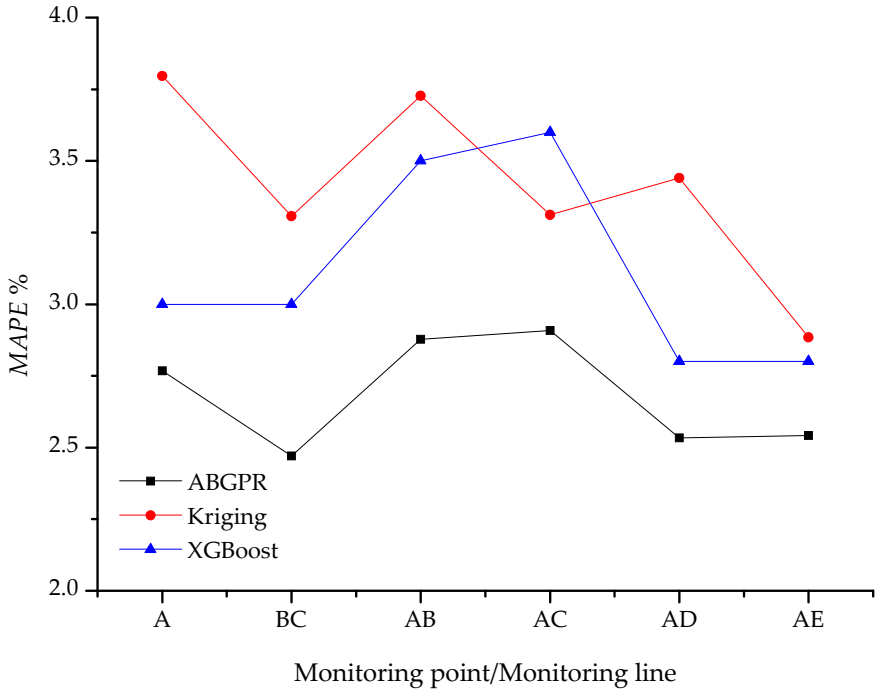

Figure 8. Comparison of *MAPE* of models based on ABGPR, Kriging and XGBoost.

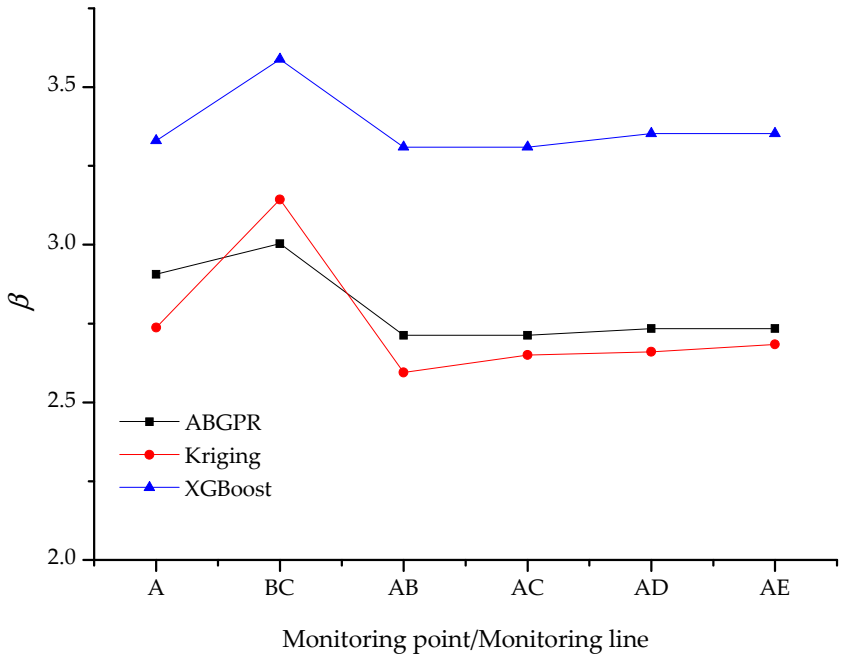

Figure 9. Comparison of tunnel reliability based on ABGPR, Kriging and XGBoost.

From Figure 8, we note that for monitoring point A and monitoring lines BC, AB, AC, AD and AE, the *MAPE* values of ABGPR-based surrogate models fluctuate between 2.471% and 2.908%; the *MAPE* values of Kriging-based surrogate models fluctuate between 2.885% and 3.796%; the *MAPE* values of XGBoost-based surrogate models fluctuate between 2.8% and 3.6%. Furthermore, the ABGPR-based *MAPE* values of each measuring point/line are much smaller than the Kriging-based results or the XGBoost-based results.

From Figure 9, we note that the ABGPR-based reliability indices are relatively close to the Kriging-based results and differ significantly from the XGBoost-based results. The

ABGP-based reliability indices of monitoring lines AB and AC or AD and AE are not changed. Due to the symmetry of monitoring lines AB and AC or AD and AE, the reliability indices of monitoring lines AB and AC or AD and AE should be the same, but there are some changes in their Kriging-based results.

In this research, three GPR combined kernel functions were developed and compared to the basic kernel functions to determine the best GPR kernel function for the reliability analysis of deep soft rock tunnels. The Adam algorithm was also used to optimize the surrogate model's hyperparameters.

Although GPR is a non-parametric model like the Kriging method, the difference between GPR and the Kriging method is that the former assumes that the random field is a Gaussian process and provides a complete distribution of the test sample; the latter assumes that the random field is an inherently stationary process and provides its optimal unbiased estimate for the test sample. Moreover, the Kriging model, as an interpolation model, is very sensitive to noisy data. Furthermore, XGBoost cannot directly identify the interaction between data features at all, and there is a risk of inaccurate predictions if the feature distribution of the prediction set is different from that of the original training set. Therefore, among the ABGPR method, the Kriging method, and the XGBoost method, the ABGPR-based $R2$_score is the largest, the ABGPR-based MAPE is the smallest, and the fluctuation in the ABGPR-based calculation results is also the smallest. The advantages of the proposed method are that its prediction error is the smallest and its prediction ability is the strongest among the ABGPR method, the Kriging method, and the XGBoost method.

It should be noted especially that if the data point number is insufficient or unevenly distributed, it may lead to inaccurate Kriging interpolation results. In addition, if the assumption that data have spatial correlation is not valid, the Kriging interpolation results may be affected. The XGBoost model may overfit, especially when the dataset is small or there are many features. And, for completely missing features, the XGBoost model may not be able to effectively learn the importance of these features, thereby affecting the performance of the model.

3.4.4. Comparison with the Polynomial Response Surface Method and ABGPR-MCS

The methods for solving the random reliability (the proposed framework) and the response surface reliability are completely different. Generally, the random reliability can be regarded as an exact solution, while response surface reliability can be regarded as an approximate solution.

For the support structure of the tunnel, in order to further investigate the efficiency and feasibility of the obtained reliability indices, and considering the characteristics that the structural performance function cannot be explicitly expressed in the research problem, we use the polynomial response surface method (PRSM) to calculate the structural reliability. In the PRSM, we select sampling points using the star design method, and each calculation step needs to calculate the values of sampling points through FEM simulation.

When the response surface method (RSM) [34] is used to calculate the structural reliability index, the calculation of the reliability index becomes an optimization problem, as shown in Formula (19).

$$\beta = \min_{\overline{g}(x)=0} \sqrt{\boldsymbol{n}^T \boldsymbol{R}^{-1} \boldsymbol{n}} \tag{19}$$

where $\overline{g}(x)$ is the polynomial expression of the performance function; $\boldsymbol{R}$ is the correlation coefficient matrix of a random variable $\boldsymbol{x}$; $\boldsymbol{R}$ is taken as the unit matrix in this study; $\boldsymbol{n}$ represents the degenerate space vector corresponding to $\boldsymbol{x}$.

The final solving process of PRSM can be carried out with the help of the planning solver tool in Excel 2021. The iteration results are shown in Table 4. The reliability indices of two iteration steps before and after and the change in the step size of checkpoints in Table 4 are compared. It is determined that the calculation of the PRSM is converged when the number of iterations reaches nine. Taking the average value of the reliability indices

of iteration steps 8 and 9 as the result, the reliability index of the tunnel vault structure is obtained as 2.70.

Table 4. Iteration results of PRSM.

Iteration Number	*E*/GPa	μ	*c*/MPa	φ/°	β
0	0.3306	0.338	0.1896	32.795	
1	0.3271	0.338	0.1874	32.483	2.87
2	0.3288	0.338	0.1864	32.424	2.94
3	0.3281	0.338	0.1864	32.507	2.77
4	0.3291	0.338	0.1860	32.484	2.80
5	0.3287	0.338	0.1863	32.491	2.77
6	0.3288	0.338	0.1863	32.514	2.64
7	0.3284	0.338	0.1867	32.560	2.40
8	0.3278	0.338	0.1873	32.480	2.68
9	0.3288	0.338	0.1864	32.484	2.71

The result of tunnel structure reliability obtained using the PRSM (2.7) is close to the result obtained using the ABGPR-MCS reliability method (2.906), which shows that the proposed method is efficient and feasible.

3.4.5. Comprehensive System Reliability Index of Tunnel Structure

The system reliability is usually adopted to estimate the failure probability range of a structural system. Assuming that the failure of each part of a soft rock tunnel structure is completely related, the failure probability of a tunnel section may be denoted as Formula (20).

$$p_{\text{f_lower}} = \max(p_{\text{f1}}, p_{\text{f2}}, \ldots p_{\text{fn}}) \tag{20}$$

From Formula (20), we can obtain the minimum failure probability of the tunnel as $p_{\text{f_lower}}$ = 0.333%.

Assuming that the failure of the tunnel for each element is independent, its corresponding displacement failure probability may be expressed as Formula (21). From Formula (21), we can obtain the maximum failure probability of the tunnel $p_{\text{f_upper}}$ = 0.96%.

$$p_{\text{f_upper}} = 1 - \prod_{i=1}^{n} (1 - p_{\text{f}i}) \tag{21}$$

Thus, the final failure probability of the tunnel initial support structure system in this study is between $p_{\text{f_lower}}$ and $p_{\text{f_upper}}$, and may be expressed as Formula (22).

$$0.333\% \leq P_{\text{f}} \leq 0.96\% \tag{22}$$

As the range of $p_{\text{f_lower}}$ and $p_{\text{f_upper}}$ is very small, only 0.6465%, their average value, can be taken as the point estimate value, and its corresponding comprehensive reliability is 2.486.

4. Conclusions

The ABGPR-MC reliability method of an initial support structure for a deep rock tunnel was proposed in this study. The LHS method was employed to generate the sampling points for obtaining the geo-mechanical parameter dataset of the ABGPR. CRBF was constructed and selected as the kernel function in the ABGPR-MCS reliability calculation. The efficiency and feasibility of the proposed method were illustrated and analyzed by ABGPR-MC and PRSM. The conclusions are as follows.

1. A comparison among the prediction abilities of RBF, K1.5, K2.5, RBFK1.5, RBFK2.5, and CRBF indicates that the prediction ability of CRBF is the strongest. It is denoted

that the prediction ability of the ABGP model can be greatly improved through the design of the combined kernel functions.

2. A comparison between the reliability indices obtained from the proposed ABGPR-MCS method and the PRSM indicates that ABGPR-MCS is an efficient method for the probabilistic analyses of deep rock tunnel engineering. The most distinct advantage of the proposed method is that it can establish an optimized surrogate model for the numerical simulation calculation and obtain the mean value, variance, and confidence interval of geo-mechanical parameters.
3. For deep rock tunnel structure systems with fewer failure elements, using the proposed ABGPR-MCS reliability analysis method and the system reliability theory can estimate its failure probability range and determine its comprehensive reliability index. The proposed method can quickly assess the chances of large deformation disasters in deep soft rock non-circular tunnels.
4. From the system reliability calculation results obtained by using the proposed reliability method, it can be denoted that the support structure of the tunnel in this study is safe, which is consistent with the actual situation. For zones of the initial support structure of the tunnel with low reliability, the reliability and safety of the tunnel can be improved by strengthening the initial support measures.
5. Using the ABGPR method to establish a surrogate model of the nonlinear mapping relationship between geo-mechanical parameters and their responses can significantly reduce the time needed for numerical simulation calculations. There are obvious advantages regarding the prediction error and the prediction ability of the proposed method (ABGPR) compared with Kriging and XGBoost.

The selection of kernel functions in this study mainly considers model performance, and the next step of research needs to combine data characteristics, computational resources, and parameter adjustments.

Due to the fact that it took over two months for more than 1000 rounds of 3D numerical simulation calculations by using ABAQUS, we only conducted sampling using the LHS method in this study. In further research, we will incorporate a bootstrapping technique to conduct the sampling to eliminate the effect of randomness in DoE.

The dynamic loads and weakening of the rock mass due to the presence of water have a significant impact on the stability of deep-buried soft rock tunnels. Our numerical simulation did not consider them, which is the main limitation of this study. We will conduct a further study on whether the proposed method is applicable to the two above-mentioned working conditions.

Author Contributions: J.X.: conceptualization, formal analysis, writing—review and editing, funding acquisition, supervision, investigation, resources; Z.Y.: software; Y.W.: formal analysis. All authors have read and agreed to the published version of the manuscript.

Funding: This research was funded by the China Postdoctoral Science Foundation, grant number 20060390165.

Institutional Review Board Statement: Not applicable.

Informed Consent Statement: Not applicable.

Data Availability Statement: Data are contained within this article. Due to intellectual property rights, the data provided in this study can be provided on request to the corresponding author.

Conflicts of Interest: The authors declare no conflict of interest.

References

1. Pan, Q.J.; Dias, D. An efficient reliability method combining adaptive support vector machine and Monte Carlo Simulation. *Struct. Saf.* **2017**, *67*, 85–95. [CrossRef]
2. Feng, L.Y.; Zhang, L.M. Reliability–based multi–objective optimization in tunneling alignment under uncertainty. *Struct. Multidisc. Optim.* **2021**, *63*, 3007–3025. [CrossRef]

3. Liu, W.; Chen, E.; Yao, E.; Wang, Y.; Chen, Y. Reliability analysis of face stability for tunnel excavation in a dependent system. *Reliab. Eng. Syst. Saf.* **2021**, *206*, 107306. [CrossRef]
4. Xu, Z.Y.; Saleh, J.H. Machine learning for reliability engineering and safety applications: Review of current status and future opportunities. *Reliab. Eng. Syst. Saf.* **2021**, *211*, 107530. [CrossRef]
5. Wang, Z.L.; Zhao, D.Y.; Guan, Y. Flexible–constrained time–variant hybrid reliability–based design optimization. *Struct. Multidisc. Optim.* **2023**, *66*, 89. [CrossRef]
6. Wang, Q.; Fang, H.B. Reliability analysis of tunnels using an adaptive RBF and a first–order reliability method. *Comput. Geotech.* **2018**, *98*, 144–152. [CrossRef]
7. Chakraborty, S.; Majumder, D. Hybrid reliability analysis framework for reliability analysis of tunnels. *J. Comput. Civ. Eng.* **2018**, *32*, 04018018. [CrossRef]
8. da Silva, C.C.C.; Bernaud, D.; Real, M.D.; Maghous, S. Reliability analysis of bolt-supported tunnels regarded as homogenized structures. *Int. J. Numer. Anal. Methods Geomech.* **2023**, *47*, 2531–2561. [CrossRef]
9. Do, D.P.; Vu, M.N.; Tran, N.T.; Armand, G. Closed-form solution and reliability analysis of deep tunnel supported by a concrete liner and a covered compressible layer within the viscoelastic Burger rock. *Rock Mech. Rock Eng.* **2021**, *54*, 2311–2334. [CrossRef]
10. Wang, Q.; Huang, T.C. Time-variant reliability analysis of underground structures against delayed failure based on the probability density evolution method. *Eng. Fail. Anal.* **2022**, *142*, 106695. [CrossRef]
11. Xu, J.C.; Sun, C.; Rui, G.R. NSGA–III–XGBoost–based stochastic reliability analysis of deep soft rock tunnel. *Appl. Sci.* **2024**, *14*, 2127. [CrossRef]
12. Lü, Q.; Chan, C.L.; Low, B.K. System reliability assessment for a rock tunnel with multiple failure modes. *Rock Mech. Rock Eng.* **2013**, *46*, 821–833. [CrossRef]
13. Zhao, H.B. High dimension model representation–based response surface for reliability analysis of tunnel. *Math. Probl. Eng.* **2018**, *2018*, 8049139. [CrossRef]
14. Zhao, H.B.; Ru, Z.L.; Chang, X.; Yin, S.D.; Li, S.J. Reliability analysis of tunnel using least square support vector machine. *Tunn. Undergr. Space Technol.* **2014**, *41*, 14–23. [CrossRef]
15. Zhou, S.Y.; Guo, X.F.; Zhang, Q.; Dias, D.; Pan, Q.J. Influence of a weak layer on the tunnel face stability—Reliability and sensitivity analysis. *Comput. Geotech.* **2020**, *122*, 103507. [CrossRef]
16. Wang, Q.; Fang, H.B.; Shen, L. Reliability analysis of tunnels using a metamodeling technique based on augmented radial basis functions. *Tunn. Undergr. Space Technol.* **2016**, *56*, 45–53. [CrossRef]
17. Feng, L.Y.; Zhang, L.M. Assessment of tunnel face stability subjected to an adjacent tunnel. *Reliab. Eng. Syst. Saf.* **2021**, *205*, 107228. [CrossRef]
18. Xu, J.C.; Jiang, Y.; Yang, C.B. Landslide displacement prediction during the sliding process using XGBoost, SVR and RNNs. *Appl. Sci.* **2022**, *12*, 6056. [CrossRef]
19. Yan, Y.H.; Li, X.R.; Sun, W.J.; Fang, X.; He, F.J.; Tu, J.Y. Semi–surrogate modelling of droplets evaporation process via XGBoost integrated CFD simulations. *Sci. Total Environ.* **2023**, *895*, 164968. [CrossRef]
20. Wang, Y.; Gao, Y.; Liu, Y. Bayesian–entropy gaussian process for constrained metamodeling. *Reliab. Eng. Syst. Saf.* **2021**, *214*, 107762. [CrossRef]
21. Li, T.Z.; Dias, D. Tunnel face reliability analysis using active learning Kriging model–Case of a two–layer soils. *J. Cent. South Univ.* **2019**, *26*, 1735–1746. [CrossRef]
22. Langford, J.C.; Diederichs, M.S. Reliability based approach to tunnel lining design using a modified point estimate method. *Int. J. Rock Mech. Min.* **2013**, *60*, 263–276. [CrossRef]
23. Jerez, D.J.; Jensen, H.A.; Beer, M. An effective implementation of reliability methods for Bayesian model updating of structural dynamic models with multiple uncertain parameters. *Reliab. Eng. Syst. Saf.* **2022**, *225*, 108634. [CrossRef]
24. Liu, H.; Low, B.K. System reliability analysis of tunnels reinforced by rockbolts. *Tunn. Undergr. Space Technol.* **2017**, *65*, 155–166. [CrossRef]
25. Ji, J.; Zhang, Z.; Wu, Z. An efficient probabilistic design approach for tunnel face stability by inverse reliability analysis. *Geosci. Front.* **2021**, *12*, 380–389. [CrossRef]
26. Hamdia, K.M.; Ghasemi, H. Reliability analysis of the stress intensity factor using multilevel Monte Carlo methods. *Probabilistic Eng. Mech.* **2023**, *74*, 103497. [CrossRef]
27. Sadr, M.; Torrilhon, M.; Gorji, M.H. Gaussian process regression for maximum entropy distribution. *J. Comput. Phys.* **2020**, *418*, 109644. [CrossRef]
28. Kingma, D.P.; Ba, J.L. Adam: A method for stochastic optimization. In Proceedings of the 3rd International Conference on Learning Representations, San Diego, CA, USA, 7–9 May 2015.
29. Contreras, L.F.; Brown, E.T. Slope reliability and back analysis of failure with geotechnical parameters estimated using Bayesian inference. *J. Rock Mech. Geotech. Eng.* **2019**, *11*, 628–643. [CrossRef]
30. Rasmussen, C.E.; Williams, C.K.I. *Gaussian Processes for Machine Learning*; MIT Press: Cambridge, MA, USA, 2006.
31. Fitzgerald, D.L. Statistical aspects of Tricomi's function and modified Bessel functions of the second kind. *Stoch. Environ. Res. Risk Assess.* **2000**, *14*, 139–158. [CrossRef]
32. Griffiths, D.; Fenton, G. *Risk Assessment in Geotechnical Engineering*; John Wiley & Sons: Hoboken, NJ, USA, 2008.

33. Lophaven, S.N.; Nielsen, H.B.; Sondergaard, J. *DACE: A MATLAB Kriging Toolbox, Tech. Rep. IMM-TR-2002-12*; Technical University of Denmark: Kongens Lyngby, Denmark, 2002.
34. Gunst, R. Response surface methodology: Process and product optimization using designed experiments. *Technometrics* **2008**, *38*, 284–286. [CrossRef]

Disclaimer/Publisher's Note: The statements, opinions and data contained in all publications are solely those of the individual author(s) and contributor(s) and not of MDPI and/or the editor(s). MDPI and/or the editor(s) disclaim responsibility for any injury to people or property resulting from any ideas, methods, instructions or products referred to in the content.